

USE OF A PROBABILISTIC SHAPE MODEL FOR NON-LINEAR REGISTRATION OF 3D SCATTERED DATA

Isabelle Corouge, Christian Barillot

Irisa, Campus de Beaulieu, 35042 Rennes Cedex, France

Email : icorouge@irisa.fr

ABSTRACT

In this paper we address the problem of registering 3D scattered data by the mean of a statistical shape model. This model is built from a training set on which a principal component analysis (PCA) is applied. A local system of reference is computed for each sample shape of the learning set, what enables to align the training set. PCA then reveals the main modes of deformation of the class of objects of interest. Furthermore, the deformation field obtained between a given shape and a reference shape is extended to a local neighborhood of these shapes by using an interpolation based on the thin-plate splines. It is then used to register objects associated with these shapes in a local and non-linear way. The data involved here are cerebral data both anatomical (cortical sulci) and functional (MEG dipoles).

1. INTRODUCTION

Within the scope of three-dimensional cerebral imaging we are more particularly interested in anatomo-functional normalization. We aim at merging scattered data from various subjects and/or acquired according to various modalities (*e.g.* magnetic resonance imaging (MRI) for anatomical data, magnetoencephalography (MEG) or functional magnetic resonance imaging (fMRI) for functional data). The strong inter-individual variability implied by such data can be grasped by a shape model. Deformable models are a powerful tool to image analysis [1]. Some of them use modal analysis technique lying on a physical approach [2, 3] or on a statistical approach [4, 5, 6]. In this kind of model, adequation between model and data is improved by introducing *prior* knowledge thanks to a training set. These models are able not only to represent the shape of an object but also the way it can vary. They are generally used for segmentation purpose. Within the framework of anatomo-functional normalization it is interesting to use the modeling of deformations to register scattered data associated with

Thanks to Regional Council for Brittany, the GIS (“Groupement d’Intérêt Scientifique”) “Sciences de la Cognition”, the Montreal Neurological Institute, Canada and the Signal and Images in Medicine laboratory, Rennes, France.

modeled structures of interest. With this aim a technique based on thin-plate splines interpolation is considered [7, 8].

In this paper, we treat multi-subjects MRI/MEG scattered data. We model particular anatomical structures: the cerebral cortex sulci, and use this modeling to register MEG dipoles (localizations of functional activity). We describe in section 2 the construction of the statistical model of cortical sulci by learning a set of shapes. The training stage is first detailed, then we present the statistical analysis we use, *i.e.* the principal component analysis (PCA). In section 3 we present the thin-plate spline method and its use combined to the model exploitation in the local and non-linear registration of MEG dipoles.

2. STATISTICAL MODEL OF CORTICAL SULCI

2.1. Training

The training set consists of typical shapes of the class of objects to study. We are interested here in cortical sulci which are anatomical structures whose shape is complex. We dispose of a parametric representation of these shapes of interest [9], describing them by their median surface. This one is extracted from MRI volumes by the “active ribbon” method and is eventually modeled by a cubic B-spline surface, which is a well adapted modeling to free form objects. The spline, parameterized by u and v , is described by nbp knots and $nbc = nbc_u * nbc_v$ control points where nbc_u (resp. nbc_v) is the number of control points in the direction associated with the parameter u (resp. v). In the case of sulci, the parametric direction u represents the length of the sulcus and the direction v its depth. Giving nbc control points completely defines the sulcal surface. Consequently, we can represent a sulcus by the vector of its knots or its control points. The ratio nbc/nbp defines the smoothing factor: the smaller this ratio, the smoother the surface (here $nbc/nbp = 1/24$). The main advantages to use control points are their lower number and their complete representation of each surface.

The statistical technique used here needs to establish the point to point correspondences between all shapes of the

training set. This implies a resampling stage so that the sulci have the same number of points and a registration stage in order to express them in the same system of reference. Each sulcus is initially expressed in its image referential system which is different from one patient to another. The idea is to associate its own system of reference with each sulcus, built so that it is common to all sulci. We call it “local system of reference”. It is then just needed to determine the rigid transformation (rotation+translation) aligning all local systems of axes and to apply it to the associated shapes.

Let $\mathcal{R}_s(O_s, \mathbf{u}_s, \mathbf{v}_s, \mathbf{w}_s)$ be the system of reference local to the sulcus. The axes \mathbf{u}_s , \mathbf{v}_s and \mathbf{w}_s are defined as the axes of inertia of the sulcal surface, and are decided to be so that \mathbf{u}_s follows the length of the sulcus, \mathbf{v}_s its depth and \mathbf{w}_s its normal. This discrimination between the 3 axes is first carried out by considering that \mathbf{u}_s (resp. \mathbf{v}_s) is the axis of inertia the “most collinear” with the *nbc_u* (resp. *nbc_v*) pseudo-parallel directions ; each of them being defined by the two extremities of a sulcus’ line in direction *u* (resp. *v*). Then \mathbf{w}_s is obtained by vector product: $\mathbf{w}_s = (\mathbf{u}_s \wedge \mathbf{v}_s)$. At last the origin O_s is the center of mass of the sulcus.

The sulci have now to be expressed in their local systems of reference. It amounts to determining for each sulcus the matrix \mathbf{M} defining the change of basis from the local system of reference \mathcal{R}_s towards the image system of reference, let it be $\mathcal{R}(O, \mathbf{u}, \mathbf{v}, \mathbf{w})$. Let \mathbf{R} and \mathbf{t} be the rotation matrix and the translation vector of the inverse change of basis \mathbf{M}^{-1} (*i.e.* from \mathcal{R} towards \mathcal{R}_s). Then in homogeneous coordinates:

$$\mathbf{R} = \begin{pmatrix} \mathbf{u}_s & \mathbf{v}_s & \mathbf{w}_s \end{pmatrix}, \mathbf{t} = \overrightarrow{OO_s} \text{ and } \mathbf{M}^{-1} = \begin{pmatrix} \mathbf{R} & \mathbf{t} \\ 0 & 0 & 0 & 1 \end{pmatrix}$$

$$\text{Since } \mathbf{R} \text{ orthogonal: } \mathbf{M} = \begin{pmatrix} \mathbf{R}^T & -\mathbf{R}^T \mathbf{t} \\ 0 & 0 & 0 & 1 \end{pmatrix}$$

Applying this rigid transformation to all the points of each sulcus aligns the training set as illustrated on figure 1. No homothety is necessary since the image data are acquired to the same scale.

The next stage consists in resampling the sulci of the training set. We resample the elements of the training population on the one which has the most sample points, spline properties ensuring that the original shapes are preserved. Once the sulci are resampled and aligned, the matching is performed by just assigning control point to control point according to their curvilinear abscissa.

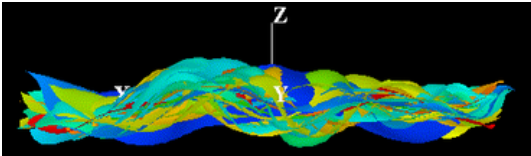


Fig. 1. A side view of a database of 18 left central sulci aligned in the local system of reference.

2.2. Statistical Analysis of Deformations

The statistical analysis of the training set leads to a modeling of cortical sulci and of their variations. The model captures the shape variability observed within the training set. Indeed, the statistical analysis reveals the main modes of variation relative to a prototype shape, representative of the considered class. We use a principal component analysis which enables to represent data in a new basis, orthogonal, and which suppresses the redundancy of information. Moreover, this analysis enables a modal approximation.

2.2.1. Principal Component Analysis

Let \mathcal{P} be the training population made up of N elements, $\mathbf{x}_i \in \mathcal{P}$ a shape, $\bar{\mathbf{x}}$ the mean shape on \mathcal{P} , \mathbf{C} the covariance matrix. A shape \mathbf{x}_i is represented by the vector of control points of the spline which models the median surface of the sulcus:

$$\mathbf{x}_i = (x_{i_1}, y_{i_1}, z_{i_1}, \dots, x_{i_n}, y_{i_n}, z_{i_n})^T \text{ with } n = nbc$$

The mean shape $\bar{\mathbf{x}}$, representative of the studied class, and the covariance matrix \mathbf{C} are given by:

$$\bar{\mathbf{x}} = \frac{1}{N} \sum_{i=1}^N \mathbf{x}_i \text{ and } \mathbf{C} = \frac{1}{N} \sum_{i=1}^N d\mathbf{x}_i d\mathbf{x}_i^T \text{ with } d\mathbf{x}_i = \mathbf{x}_i - \bar{\mathbf{x}}$$

Diagonalize the covariance matrix \mathbf{C} provides the new modal basis Φ :

$$\mathbf{C} = \Phi \Lambda \Phi^T,$$

$$\text{with } \Lambda = \text{diag}(\lambda_1, \dots, \lambda_{3n}) \text{ and } \lambda_1 \geq \lambda_2 \geq \dots \geq \lambda_{3n}$$

Then any shape \mathbf{x} can be written: $\mathbf{x} = \bar{\mathbf{x}} + \Phi \mathbf{b}$ where $\mathbf{b} = (b_1, \dots, b_{3n})^T$ is the vector of modal amplitudes of deformation and $(-\Phi \mathbf{b})$ corresponds to the deformation vectors in each point of \mathbf{x} towards the mean shape. Since the eigenvalue λ_i is the variance explained by the i^{th} mode, a large part of the variability can be explained by retaining only the first m modes. The value m is chosen so that $\sum_{i=1}^m \lambda_i$, the variance explained by the first m modes, represents a proportion, sufficiently important of the whole variance: $\lambda_T = \sum_{i=1}^{3n} \lambda_i$. Retaining only m modes enables to achieve a modal approximation:

$$\begin{cases} \mathbf{x} = \bar{\mathbf{x}} + \Phi_m \mathbf{b}_m \\ \mathbf{b}_m = \Phi_m^T (\mathbf{x} - \bar{\mathbf{x}}) \end{cases}$$

where Φ_m is a submatrix of Φ containing the first m eigenvectors of \mathbf{C} , thus defining the modal approximation basis. The vector $\mathbf{b}_m = (b_1, \dots, b_m)^T$ represents a shape in the m -dimensional space defined by the principal components. This space is interesting since it is of lower dimension (dim m). However, \mathbf{b}_m must be constrained in order to represent an “allowable” shape (*i.e.* a shape consistent with the learnt shapes). Given the assumption that the distribution of vectors \mathbf{x}_i is normally distributed (*i.e.* gaussian distribution), the range of variability of each b_i is typically such as: $-3\sqrt{\lambda_i} \leq b_i \leq +3\sqrt{\lambda_i}$.

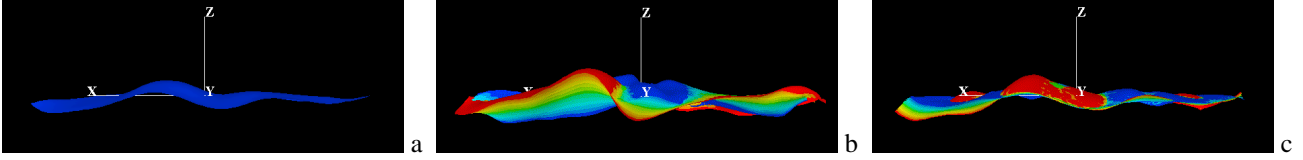


Fig. 2. a) mean sulcus, b) variations of the first mode around the mean sulcus, $-3\sqrt{\lambda_1} \leq b_1 \leq +3\sqrt{\lambda_1}$, c) variations of the 15th mode around the mean sulcus, $-3\sqrt{\lambda_{15}} \leq b_{15} \leq +3\sqrt{\lambda_{15}}$.

2.2.2. Results

Several tests have been carried out by making the cardinal of the training population varied (up to 85 sulci) and also by changing the type of sulci (central right and left sulcus, sylvian sulcus, superior frontal sulcus, . . .). We present the results obtained on a training set made up of the 18 central left sulci registered in the previous stage. Figure 3 shows the predominance of the first modes. Indeed, the first 5 modes explain a large part of the total variation (about 70%). The first mode explains on its own almost 30% of the total variation (whereas a sulcus is described by 104 control points, that is to say 312 variables, and by more than 8000 variables if knots are considered). So the chosen modeling seems to be well appropriate to express the shapes and the variations by a very reduced number of parameters. Figure 2b shows the variations due to the first mode. They are mainly relative to the length and to the torsion of the sulcus. On the contrary, figure 2c illustrates the minor influence of the 15th mode: the deformations are hardly distinct, all the sulci are almost superimposed to the mean shape.

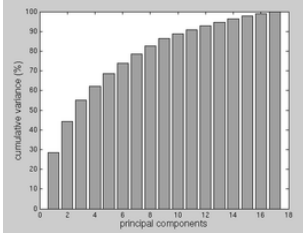


Fig. 3. Cumulative variance according to the number of principal components retained.

3. DEFORMATION FIELDS AND NON-LINEAR REGISTRATION

The deformation field $(-\Phi_{\mathbf{m}}\mathbf{b}_{\mathbf{m}})$ obtained between a given sulcus and the reference sulcus (the mean sulcus in our case) can be extended to a local neighborhood of the considered sulcus by using the thin-plate spline interpolation [10, 7]. It can then be applied to any object associated with this sulcus. We take advantage of this extension of the deformation field $(-\Phi_{\mathbf{m}}\mathbf{b}_{\mathbf{m}})$ to register scattered data located in the left central sulcus area towards a mean space.

3.1. The Thin-Plate Spline Method

Let's consider two same cardinal sets of points. The thin-plate spline method provides a mapping function between these two sets of homologous points. It associates the set of target points with the set of source points. This function is valid in some neighborhood of the set of source points. It can then be applied to a point in the source space to find its homologous in the target space.

In [7], Bookstein proposes an algebraic approach to describe deformations specified by two sets of corresponding points. The analysis lies on the function U , which is the fundamental solution of the biharmonic equation $\Delta^2 U = \delta(0, 0)$, δ being the Kronecker's function. The function U is $U(r) = |r|$ in 3D.

Let $P_i = (x_i, y_i, z_i)$, $i = 1, \dots, n$ be n source points in the Euclidean space, and $V_i = (x'_i, y'_i, z'_i)$, $i = 1, \dots, n$ be n target points. The set of points P_i describes a shape \mathbf{x} , expressed $\bar{\mathbf{x}} + \Phi_{\mathbf{m}}\mathbf{b}_{\mathbf{m}}$ according to our model. Note $r_{ij} = |P_i - P_j|$ the distance between points i and j . Define matrices:

$$\mathbf{K} = \begin{pmatrix} 0 & U(r_{12}) & \dots & U(r_{1n}) \\ U(r_{21}) & 0 & \dots & U(r_{2n}) \\ \dots & \dots & \dots & \dots \\ U(r_{n1}) & U(r_{n2}) & \dots & 0 \end{pmatrix}, \quad \mathbf{P} = \begin{pmatrix} 1 & x_1 & y_1 & z_1 \\ 1 & x_2 & y_2 & z_2 \\ \vdots & \vdots & \vdots & \vdots \\ 1 & x_n & y_n & z_n \end{pmatrix},$$

$$\mathbf{L} = \left(\begin{array}{c|c} \mathbf{K} & \mathbf{P} \\ \hline \mathbf{P}^T & \mathbf{0} \end{array} \right)$$

and the vector $\mathbf{Y} = (\mathbf{V} \mid 0 \ 0 \ 0 \ 0)^T$ where $\mathbf{V} = (v_1, \dots, v_n)$ is the vector of one coordinate of the target set (for example $\mathbf{V} = (x'_1, \dots, x'_n)$). Define eventually the vectors $\mathbf{W} = (w_1, w_2, \dots, w_n)$ and $\mathbf{a} = (a_1, a_x, a_y, a_z)$ by:

$$(\mathbf{W} \mid \mathbf{a})^T = \mathbf{L}^{-1}\mathbf{Y}$$

Regarding the target set as the mean shape $\bar{\mathbf{x}}$, the elements of $(\mathbf{W} \mid \mathbf{a})$ represent the deformation field $(-\Phi_{\mathbf{m}}\mathbf{b}_{\mathbf{m}})$ extended. They can be used to define a function f valid in a neighborhood of the source set. Thus the homologous of a point is given by:

$$f(x, y, z) = a_1 + a_x x + a_y y + a_z z + \sum_{j=1}^n w_j U(|P_j - (x, y, z)|)$$

(to decline for $f_x(x, y, z)$, $f_y(x, y, z)$, $f_z(x, y, z)$).

The affine part of f represents its behavior at infinity, the second part being asymptotically flat.

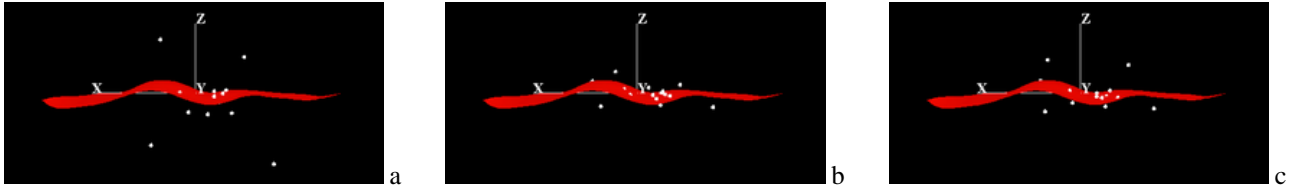


Fig. 4. Registration of MEG dipoles (somatosensory activation of the thumb): the sulcus is the mean left central sulcus. a) the dipoles are rigidly registered. b), c) the dipoles are registered via the deformation field, b) $m = 17$, c) $m = 5$.

	Rigid			TPS ($m = 17$)			TPS ($m = 5$)		
thumb	90.80	25.41	69.99	77.33	21.98	7.3	80.88	20.39	16.67
index finger	90.89	31.58	71.85	85.46	26.25	5.96	82.39	26.99	11.81
little finger	97.79	33.36	81.94	90.18	34.26	8.05	88.29	32.99	21.91

Table 1. The covariance along x , y and z of MEG dipoles for somatosensory activations (thumb, index, little finger) after rigid registration and thin-plate splines (TPS) interpolation based registration for $m = 17$ and $m = 5$.

3.2. Results

The scattered data we deal with are on one side anatomical data with cortical sulci, and on the other side functional data with MEG dipoles corresponding to a somatosensory activation of right hand fingers (thumb, index, little finger) performed for 15 of the 18 subjects of our database (see Sect. 2). Three dipoles per subject (one for each finger) are selected and are thus available. These functional activations are located in the central sulcus area. We can then jointly use the statistical modeling of cortical sulci with the thin-plate spline method to merge, in a local and non-linear way, this anatomical and functional information in the central sulcus mean space. First, we rigidly register each dipole towards the local space by applying the transformation described by the corresponding matrix \mathbf{M} (see Sect. 2). Then, for each subject, we compute the “field” ($\mathbf{W} | \mathbf{a}$) between his left central sulcus and the mean sulcus, and apply it to his three dipoles; the field ($-\Phi_m \mathbf{b}_m$) being computed with all the modes ($m = 17$). Figure 4b shows that dipoles gather around the plane of the mean sulcus. Moreover, the covariance along x , y and particularly z is considerably reduced (see Table 1). We present a second test in which we consider only 5 modes in the construction of ($-\Phi_m \mathbf{b}_m$). This approximation smoothes the sulcus and discards minor modes possibly resulting from potential segmentation errors of initial data. Results are presented Fig. 4c and Table 1. The gathering towards the mean plane and the decrease of the covariance are less than the ones of the previous test, but still significant.

4. CONCLUSION

In this paper, we have presented a local and non-linear inter-individual fusion scheme of anatomical and functional data, based both on a statistical modeling of anatomical structures, the cortical sulci, and on the use of the thin-plate spline method. The model, built by modal analysis on a training population, accounts for the sulcal variability between in-

dividuals, the achieved tests showing the relevance of the obtained deformation modes. Since this modeling lies in a “mean space”, the modeled sulci can be used as landmarks to register MEG dipoles towards the mean space. Additional experiments could be done. For instance, it would be interesting to reproject registered dipoles onto fMRI volumes. The present method can be applied to any field in computer vision where statistical models would be used to register scattered data.

5. REFERENCES

- [1] T. McInerney and D. Terzopoulos, “Deformable models in medical image analysis: A survey,” *MedIA*, vol. 1, no. 2, pp. 91–108, 1996.
- [2] G. Subsol, J.P. Thirion, and N. Ayache, “A general scheme for automatically building 3d morphometric anatomical atlases: application to a skull atlas,” *MedIA*, vol. 2, no. 1, pp. 37–60, 1998.
- [3] J. Martin, A. Pentland, S. Sclaroff, and R. Kikinis, “Characterization of neuropathological shape deformations,” *IEEE Trans. on PAMI*, vol. 20, no. 2, pp. 97–112, 1998.
- [4] C. Kervrann and F. Heitz, “A hierarchical statistical framework for the segmentation of deformable objects in image sequences,” in *IEEE CVPR*, 1994, pp. 724–728.
- [5] T.F. Cootes, C.J. Taylor, D.H. Cooper, and J. Graham, “Active shape models - their training and application,” *CVIU*, vol. 61, no. 1, pp. 38–59, 1995.
- [6] C. Nikou, H. Heitz, and J.J. Armspach, “A probabilistic multi-object deformable model for mr/spect brain image registration and segmentation,” in *SPIE Proc. of the Int. Conf. on Medical Imaging*, 1999, vol. 3361, pp. 20–26.
- [7] F. Bookstein, “Principal warps: Thin-plate splines and the decomposition of deformations,” *IEEE Trans. on PAMI*, vol. 11, no. 6, pp. 567–585, 1989.
- [8] K. Rohr, H.S. Stiehl, R. Sprengel, W. Beil, T.M. Buzug, J. Weese, and M.H. Kuhn, “Point-based elastic registration of medical image data using approximating thin-plate splines,” in *Visualization in Biomedical Computing*, 1996, pp. 297–306, Springer.
- [9] G. Le Goualher, C. Barillot, and Y. Bizais, “Modeling cortical sulci with active ribbons,” *IJPRAI*, vol. 8, no. 11, pp. 1295–1315, 1997.
- [10] J. Duchon, “Interpolation des fonctions de deux variables suivant le principe de la flexion des plaques minces,” *RAIRO Analyse Numérique*, vol. 10, pp. 5–12, 1976.